Semiconductor Junction Varactors with High Voltage-Sensitivity*

J. J. CHANG†, MEMBER, IEEE, J. H. FORSTER†, AND R. M. RYDER†, FELLOW, IEEE

Summary—For many varactor applications, structures with a large relative capacitance variation would be desirable. Two such structures have been investigated, namely, the hyperabrupt junction and the "pagoda" structure in which junction area varies with bias. All junctions are assumed to be p^+n type with an n^+ substrate, and the width of the n region is optimum, *i.e.*, completely swept out just at breakdown voltage. The series resistance is assumed to be contributed by the n region alone and is equal to the value at zero bias. Structures having equal breakdown voltages are intercompared with usual step junction varactors with respect to two figures of merit: 1) the dynamic quality factor $\tilde{Q}$ defined by Kurokawa and Uenohara for low-noise reactance amplification, and 2) the transducer gain g_T derived by Hyltin and Kotzebue for varactor harmonic generation. It is found for both applications that improvement due to increased capacitance-voltage sensitivity is offset or more than offset by the concomitant increase in RC product. For example, in the case of low-noise amplification, the improved relative capacitance variation can boost $\tilde{Q}$ by a factor of about 3 to 5, but the accompanying increase in RC product lowers Q by a factor of about 4 to 16.

However, in some cases the resistance in the junction may not be the factor which limits circuit performance. It may for instance be dominated by constant resistances such as those in the semiconductor bulk, ohmic contacts, or external circuits. In such a case the improvement in voltage sensitivity may be desirable.

I. Introduction

SEMICONDUCTOR varactor diodes have played an important role in microwave communication. The essential features of a varactor are its low shunt conductance, low series resistance and nonlinear relation between charge and voltage. Usually, low shunt conductance can easily be obtained. By using an epitaxial film and a double diffusion process, the series resistance in the semiconductor junction and bulk can be substantially reduced.[1] To increase the nonlinearity between the charge and the voltage, hyperabrupt junctions[2-5] and a pagoda structure[6] can be used. The purpose of this work is to investigate the improvement in performance, if any, that can be expected from the hyperabrupt and pagoda structures. In Section II, the hyperabrupt junction is discussed in general and the two types of hyperabrupt junctions to be discussed in this paper are introduced. Assumptions and approximations to be used in calculations are listed in Section III. Theoretical comparison between hyperabrupt junctions and abrupt junctions is made in Section IV for applications as low-noise parametric amplifiers. In Section V, hyperabrupt junctions as harmonic generators are discussed. In Section VI, varactors with a pagoda structure are introduced and the expected performance calculated. General conclusions are given in Section VII.

II. The Hyperabrupt Junction

A hyperabrupt semiconductor p-n junction is one in which the net impurity concentration decreases with the distance from the boundary between the p and n regions. Hence, it is also called a negative-gradient, reverse-graded or retrograded junction. A negative gradient may exist in the entire active region of the semiconductor or just in a part of it. The idealized impurity profile of a typical hyperabrupt junction made in an epitaxial film is shown in Fig. 1. Since the mobility of electrons is usually higher than that of holes,[7] it is desirable to choose the high resistivity side of the junction to be n type. The junction shown in Fig. 1 and all the junctions to be discussed in this work are p^+-n junctions.

The symbols used in Fig. 1 are the following:

N_a = acceptor impurity concentration in the p region
N_b = donor impurity concentration in the substrate
N_f = donor impurity concentration in the epitaxial film
N_0 = surface concentration of the donor diffusion
x_f = thickness of the epitaxial film
x_j = position of the p-n junction
x_n = space-charge region boundary on the n side at an arbitrary bias voltage. $x_{n(0)}$ is x_n at zero bias and $x_{n(bd)}$ is x_n at breakdown voltage. It is always assumed that x_f is so chosen that $x_{n(bd)} = x_f$.

* Received January 31, 1963. This work was supported in part by the United States Army Signal Corps under Contract DA 36-039 sc-85325. This paper was presented at the IRE 1962 Electron Devices Meeting, Washington, D. C.; October 25–27.

† Bell Telephone Laboratories, Inc., Murray Hill, N. J.

[1] J. J. Chang and J. H. Forster, "Diffused Epitaxial Silicon Varactors: Calculations," Bell Telephone Laboratories, Inc., 5th Interim Rept. on Microwave Solid State Devices, Contract No. DA 36-039 sc-85325, pp. 4–15; August 30, 1961.

[2] M. E. McMahon and G. F. Straube, "Voltage-sensitive semiconductor capacitor," 1958 IRE WESCON Convention Record, pt. 3, pp. 72–82.

[3] H. G. Rudenberg, "Optimum figures of merit of varactors," *Proc. Nat'l Electronics Conf.*, vol. 15, pp. 79–82; 1959.

[4] A. Shimizu and J. Nishizawa, "Alloy-diffused variable capacitor diode with large figure-of-merit," IRE Trans. on Electron Devices, vol. ED-8, pp. 370–377; September, 1961.

[5] G. Edmundson, R. Berkstresser, and V. Sils, "High Q Variable Capacitance Diodes with Extraordinary Capacitance-Voltage Dependence," presented at 1962 IRE Electron Devices Meeting, Washington, D. C.; October 25–27.

[6] A structure similar to this was discussed by C. J. Spector, "Electronically Variable Capacitors with Improved Voltage Sensitivity," Bell Telephone Laboratories, Inc., 14th Interim Tech. Rept. on Engineering Services on Transistors, Contract DA 36-039 sc-64618, pp. 67–75; October 15, 1958.

[7] D. A. Jenny, "The status of transistor research in compound semiconductors," Proc. IRE, vol. 46, pp. 959–968; June, 1958.

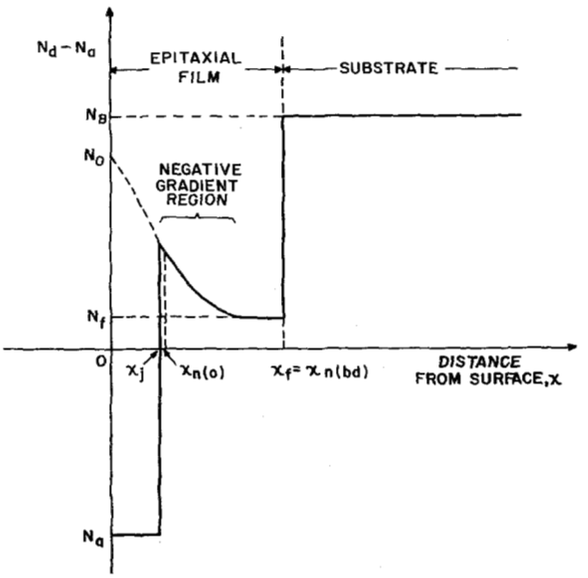

Fig. 1—Impurity profile for an epitaxial hyperabrupt junction. The magnitudes are not shown in proportion.

It is obvious that in a hyperabrupt junction the junction capacitance is more sensitive to voltage change than it is in an abrupt junction. However, this desirable increase in voltage sensitivity is accompanied by an undesirable increase in series resistance. The question thus arises as to whether a hyperabrupt junction is, in general, superior to an abrupt junction as a varactor. This will be seen to be a very involved question and we shall deal with only two particular types of hyperabrupt junctions.

As a typical case, the donor concentration N_d in the n region of a hyperabrupt junction as shown in Fig. 1 can be written as

$$N_d(x) = N_0 \exp\left[-\frac{x^2}{4D_d t_d}\right] + N_f \quad (x_j \leq x \leq x_f), \tag{1}$$

where D_d is the donor impurity diffusion coefficient and t_d is the donor diffusion time. The first term on the right-hand side of (1) represents the donor impurities diffused into the epitaxial film and the second term represents the original film doping. It is seen that $N_d(x)$ depends on four parameters, namely, N_0, x_j, $(D_d t_d)$ and N_f. How these four parameters should be chosen is an involved question. Therefore, instead of dealing with the general question of optimum impurity profile, we will consider only two particular impurity profiles. One has a very shallow negative-gradient region and differs from an abrupt junction only slightly; and the other has its negative-gradient region extended throughout the entire active part of the semiconductor and has the relation $C \propto 1/V$. They will be referred to as the type A and type B hyperabrupt junctions, respectively (Fig. 2). In the type A hyperabrupt junction, we shall further replace the negative-gradient region by a step as shown in Fig. 2(a). Thus we have

$$\begin{aligned} N_d(x) &= N, \qquad (0 \leq x \leq \delta) \\ N_d(x) &= N_f, \qquad (\delta \leq x \leq n_{x(bd)}). \end{aligned} \tag{2}$$

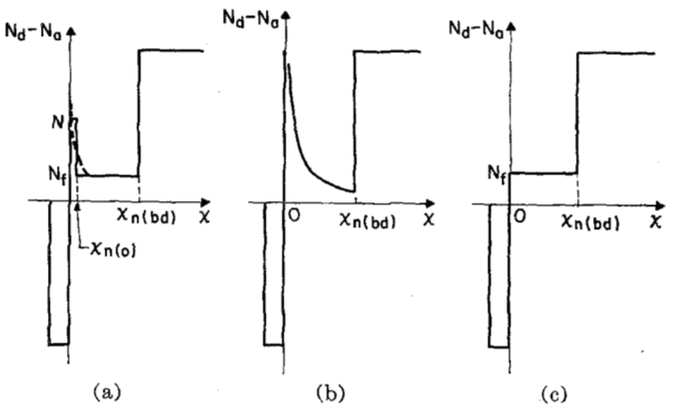

Fig. 2—Impurity profiles of the p^+-n junctions to be compared. x represents the distance from the junction. The magnitudes are not shown in proportion. (a) Type A hyperabrupt junction. (b) Type B hyperabrupt junction. (c) Abrupt junction.

Furthermore, N is chosen so that $\delta = x_{n(0)}$. Here, and from now on, the origin is chosen to be at the junction as shown in Fig. 2.

In the type B hyperabrupt junction we require that $C \propto 1/V$. Since in a highly asymmetric junction, the impurity concentration $N(x)$ on the high resistivity side can be written as a function of the junction capacitance C and the total voltage V as[8]

$$N(x) = -\frac{C^3}{\kappa q}\frac{dV}{dC}, \tag{3}$$

where κ is the dielectric constant and q is the absolute value of the electronic charge. From this relation, it can be shown that in order to have $C \propto 1/V$ in the type B hyperabrupt junction, we should have

$$N_d(x) = \frac{N_1}{x} \qquad (0 \leq x \leq x_{n(bd)}), \tag{4}$$

where N_1 is a constant. It is obvious that this type of impurity profile can only be approximated because $N_d(x)$ approaches infinity when x approaches zero. Fig. 3 shows the measured capacitance-voltage characteristics of some developmental hyperabrupt varactors. It can be seen that at low voltages, two of these curves are pretty close to what one would expect from type B hyperabrupt varactors. The breakdown voltages and the series resistances of these units at zero bias, R_0, and at a reverse bias of 6 volts, R_{-6}, are given below:

Unit No.	HV-30 No.5	HV-36 No.2	HV-46 No.2	HV-49C No.3
V_{bd} (volts)	100	62	72	7.8
R_0 (ohms)	13	5.4	2.7	2.0
R_{-6} (ohms)	3.7	2.0	0.32	1.3

The two types of hyperabrupt junctions introduced here will be used as representives of hyperabrupt junctions to be compared with abrupt junctions for applications as parametric amplifiers and harmonic generators.

[8] H. K. Henisch, "Rectifying Semiconductor Contacts," The Clarendon Press, Oxford, England, pp. 215–216; 1957.

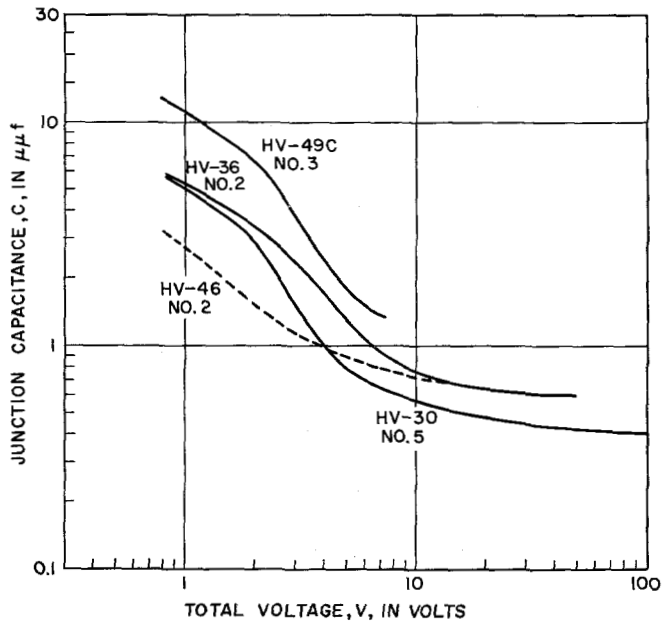

Fig. 3—The capacitance-voltage characteristics of some developmental hyperabrupt junctions measured at 1 kMc. The total voltage is the sum of the built-in potential (taken to be 0.8 volts) and the reverse bias.

III. Assumptions

The assumptions and approximations underlying the calculations to follow are listed below.

1) The doping in the p region is so much heavier than that in the n region that both the resistance and space-charge region width in the p region are negligible compared with those in the n region. Thus, with the origin at x_j the space-charge region width is simply x_n and the junction capacitance per unit area is given by

$$C = \frac{\kappa}{x_n}. \tag{5}$$

2) In the space-charge region, the impurities are completely ionized and all the mobile carriers are swept out.
3) By choosing an appropriate average value $\bar{\mu}$ for the mobility, the conductivity σ in the n region can be approximated by

$$\sigma(x) = q\bar{\mu}N_d(x), \tag{6}$$

where q is the absolute value of the electronic charge and $N_d(x)$ is the net donor impurity concentration at x.
4) The series resistance contributed by the substrate and the ohmic contacts is negligible.
5) One-dimensional treatment is valid.
6) Avalanche breakdown in the p^+-n junctions considered can be determined by the condition

$$\int_0^{x_{n(bd)}} \alpha\, dx = 1, \tag{7}$$

where[9]

$$\alpha = a \exp -\frac{b}{|E(x)|}, \tag{8}$$

and for silicon

$$a = 3.25 \times 10^6 \text{ cm}^{-1}, \tag{9}$$

and

$$b = 2.21 \times 10^6 \text{ volts/cm}. \tag{10}$$

7) Calculations are based on the properties of silicon, the built-in potential Φ is taken to be 0.8 volts, and the dielectric constant κ, $11.7/(36\pi \times 10^9)$ farad/meter.
8) In calculating the figures-of-merit, the total voltage V (sum of the applied reverse bias voltage and the built-in potential Φ) across the junction is assumed to vary from the built-in potential Φ to breakdown voltage (total) V_{bd} according to

$$V(t) = \tfrac{1}{2}[(V_{bd} + \Phi) + (V_{bd} - \Phi)\cos\omega t]. \tag{11}$$

IV. Hyperabrupt Junction Varactors as Low-Noise Parametric Amplifiers

Kurokawa and Uenohara[10] showed that the noise figure of a varactor amplifier is basically determined by a dynamic quality factor $\tilde{Q}$ as defined later in this section and the noise figure improves with increasing $\tilde{Q}$. They also showed that the open-circuit and short-circuit assumptions give the same results if the dynamic quality factor is redefined for each case. For the purpose of comparing $\tilde{Q}$ for different types of varactors, we shall calculate $\tilde{Q}$ for only one of the two definitions. Under the short-circuit assumption, $\tilde{Q}$ is defined as

$$\tilde{Q} = Q_0/(2/|\gamma_1| - |\gamma_1|/2), \tag{12}$$

where Q_0 is the average static Q of the varactor defined as

$$Q_0 = \frac{1}{\omega C_0 R_s}, \tag{13}$$

and γ_1 is defined by

$$C(t) = \frac{C_0}{2}\sum_{n=-\infty}^{\infty}\gamma_n e^{jn\omega t}\left(\begin{matrix}\gamma_0 = 2\\ \gamma_n = \gamma_{-n}\end{matrix}\right). \tag{14}$$

$C(t)$ is the junction capacitance, pumped at the angular frequency ω, and is a periodic function of time. R_s is the effective series resistance. In the calculations to follow, the series resistance at zero bias will be used instead of R_s.

The calculations of $\tilde{Q}$ for units with different V_{bd} will, in principle, follow the steps listed below:

a) Under assumption 2) and 5) one can write Gauss's law as

$$\frac{dE}{dx} = \frac{q}{\kappa}N_d(x), \tag{15}$$

[9] A. G. Chynoweth, "Ionization rates for electrons and holes in silicon," *Phys. Rev.*, vol. 109, pp. 1537–1540; March 1, 1958.
[10] K. Kurokawa and M. Uenohara, "Minimum noise figure of the variable-capacitance amplifier," *Bell Sys. Tech. J.*, vol. 40, pp. 695–722; May, 1961.

from which the electric field E can be calculated.

b) Using the result of step a) and (7) and (8) of assumption 6), one determines $x_{n(bd)}$ as a function of N_f or N_1 [see (2) and (4)].

c) The total voltage (built-in potential plus applied voltage) at avalanche breakdown determined from

$$V_{bd} = -\int_0^{x_{n(bd)}} E(x)\,dx \tag{16}$$

will also be a function of N_f or N_1.

d) Under assumptions 3) and 4) the series resistance for unit cross-sectional area at zero bias is given by

$$R_0 = \frac{1}{q\bar{\mu}} \int_{x_{n(0)}}^{x_{n(bd)}} \frac{dx}{N_d(x)}, \tag{17}$$

which will also be a function of N_f or N_1. The quantity $x_{n(0)}$ can easily be found since Φ is given in assumption (7) to be 0.8 volts.

e) From the result of step c), the capacitance-voltage relation and assumption 8), the quantities γ_1, and C_0 can be calculated.

From this calculation, $\tilde{Q}$ can be obtained and plotted against V_{bd}.

A. $\tilde{Q}$ of the Type B Hyperabrupt Junction

It can be shown that $\tilde{Q}$ of the type B hyperabrupt junction is simply

$$\tilde{Q} = \frac{1}{\omega R_0 C_{bd}} \cdot \frac{1 - \frac{\Phi}{V_{bd}}}{4}. \tag{18}$$

Following the steps outlined above, we obtain the following equation relating N_1 and $x_{n(bd)}$:

$$a x_{n(bd)} z K_1(z) = 1, \tag{19}$$

where

$$z = \left(\frac{4\kappa b}{qN_1}\right)^{1/2}, \tag{20}$$

and K_1 is the modified Bessel function of the second kind of order 1. The quantities a and b are given under assumption 6). The expressions for V_{bd} and R_0C_{bd} are

$$V_{bd} = \frac{q}{\kappa} N_1 x_{n(bd)}, \tag{21}$$

and

$$R_0 C_{bd} = \frac{\kappa}{2} \rho \left[1 - \left(\frac{\Phi}{V_{bd}}\right)^2\right], \tag{22}$$

respectively, where ρ is given by

$$\frac{1}{\rho} = q\bar{\mu} \frac{N_1}{x_{n(bd)}}. \tag{23}$$

The mobility μ is usually higher at lower impurity concentrations.[11] We shall take ρ as the resistivity corresponding to a donor concentration of $N_1/x_{n(bd)}$. This will make R_0C_{bd} slightly lower than its actual value. Even so, we shall see that the quantity $\tilde{Q}$ of this type of varactor is still much lower than that of the abrupt junction varactors. By using the above results, $\tilde{Q}$ of the type B hyperabrupt junction is calculated for *Si* and plotted in Fig. 4. The calculated $\tilde{Q}$ increases much more rapidly with decreasing breakdown voltage than that obtained experimentally. This is because the ohmic contact resistance and bulk resistance in low-voltage units cannot be neglected compared with the resistance in the p-n junction.

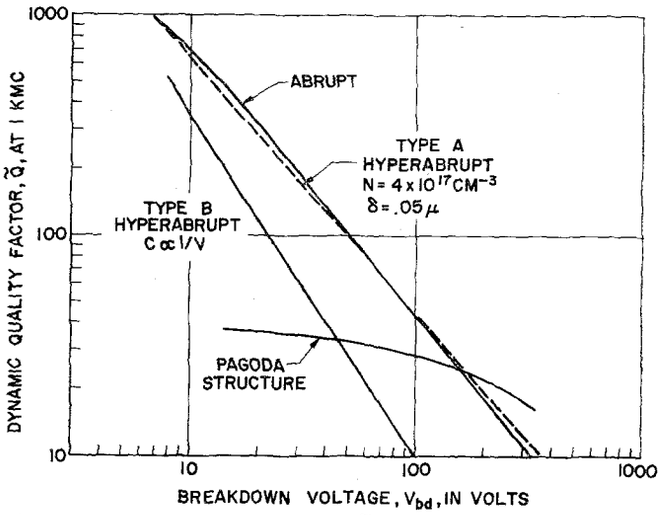

Fig. 4—The dynamic quality factor $\tilde{Q}$ at 1 kMc. The curve for the pagoda structure actually represents $\tilde{Q}_{max}$ defined by (39).

B. $\tilde{Q}$ of the Abrupt and the Type A Hyperabrupt Junctions

It can be shown that the junction capacitance of the type A hyperabrupt junction is simply

$$C = \left(\frac{qN_f}{2\kappa}\right)^{1/2} \left(V_a + \frac{N_f}{N}\Phi\right)^{-1/2}. \tag{24}$$

This is the same as that of an abrupt junction except the factor N_f/N. Therefore the computation of $\tilde{Q}$ for the type A hyperabrupt junction is similar to that for the abrupt junction and we shall discuss these two cases together. The reader is to be reminded here that the concentration N for the type A hyperabrupt junction is chosen so that $\delta = x_{n(0)}$, *i.e.*, δ and N are related by

$$\Phi = \frac{q}{2\kappa} N\delta^2. \tag{25}$$

When N is chosen to be equal to N_f, the type A hyperabrupt junction becomes an abrupt junction. For the type A hyperabrupt junction, the relation between N_f and $x_{n(bd)}$ is given by

$$\frac{ab\kappa}{q}\left[\frac{1}{N_f} - \frac{1}{N}\right] F_3(z_1) + \frac{ab\kappa}{qN} F_3(z_1 + c_1) = 1, \tag{26}$$

where z_1, c_1 and the function $F_3(z)$ are defined as

$$z_1 = \frac{qN_f}{b\kappa}\,[x_{n(bd)} - \delta], \tag{27}$$

$$c_1 = \frac{qN}{b\kappa}\,\delta, \tag{28}$$

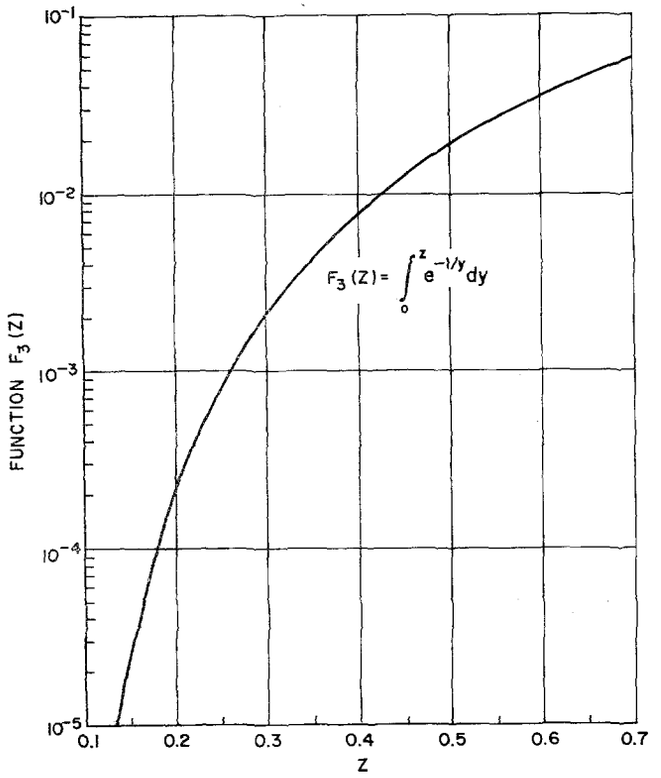

Fig. 5—Function $F_3(z)$.

and

$$F_3(z) = \int_0^z e^{-1/y} \, dy, \tag{29}$$

respectively. A plot of $F_3(z)$ is given in Fig. 5. In (26), a, b, q, and κ are constants. Either N or δ can be considered as a third parameter and is to be chosen. The total voltage at avalanche breakdown is

$$V_{bd} = \frac{q}{2\kappa} [N_f(x_{n(bd)}^2 - \delta^2) + N\delta^2]. \tag{30}$$

C_0 and R_0C_{bd} are given by

$$C_0 = \frac{2}{\pi} C_{bd}K, \tag{31}$$

and

$$R_0C_{bd} = \kappa\rho\left[1 - \frac{\delta}{x_{n(bd)}}\right], \tag{32}$$

respectively, where K in (31) is the complete elliptic integral of the first kind and ρ in (32) is the resistivity corresponding to a donor concentration of N_f.[11] The quantity $|\gamma_1|$ is given by

$$|\gamma_1| = 2\left[\frac{2(1 - \mathcal{E}/K)}{\sin^2\theta} - 1\right], \tag{33}$$

where $\mathcal{E}$ is the complete elliptic integral of the second kind and θ is defined by

$$\theta = \cos^{-1}\frac{\delta}{x_{n(bd)}}. \tag{34}$$

By using these formulas, $\tilde{Q}$ of the type A hyperabrupt junctions ($N \neq N_f$) and the abrupt junctions ($N = N_f$) are calculated for Si and plotted in Fig. 4.

From Fig. 4, the following can be seen. When the negative-gradient region of a hyperabrupt junction is very shallow, the quantity $\tilde{Q}$ is essentially the same as that of an abrupt junction, *i.e.*, the improvement in $\tilde{Q}$ due to the improvement in $|\gamma_1|$ is just about balanced out by the increase in R_0C_0. When the negative-gradient region is wide as in a type B hyperabrupt junction, the dynamic quality factor is considerably lower than that of an abrupt junction.

However, when the loss in the diode is negligible compared with the loss in the external circuits, improvement in γ_1 by using hyperabrupt junctions is believed to be desirable. Similarly, when the series resistance of the varactor is mainly contributed by constant resistances such as contact and bulk resistances, hyperabrupt junctions may also be preferable.

V. Hyperabrupt Junction Varactors as Harmonic Generators

Although many authors have analyzed the varactor diode harmonic generator, the analysis by Hyltin and Kotzebue[12] is most readily applicable to hyperabrupt junctions. Their formula for the transducer gain g_T of an nth harmonic generator says

$$g_T = \left[1 - \frac{\gamma_{n+1}}{\gamma_{n-1}}\right] \frac{\bar{\gamma}^2 Q_n^2}{[1 + (1 + \bar{\gamma}^2 Q_n^2)^{1/2}]^2}, \tag{35}$$

where

$$Q_n = \frac{1}{n\omega C_0 R_s}, \tag{36}$$

and

$$\bar{\gamma}^2 = \left[1 - \frac{\gamma_{n+1}}{\gamma_{n-1}}\right]\left[\frac{\gamma_{n-1}}{2 - \gamma_2}\right]^2. \tag{37}$$

The quantities R_s, C_0, and γ_n were defined earlier in Section IV. When the capacitance is more sensitive to voltage variation, the coefficients γ_n are larger and decrease more slowly as n increases. Thus the factor $(1 - \gamma_{n+1}/\gamma_{n-1})$ in (35) and (37) is smaller and the factor $[\gamma_{n-1}/(2 - \gamma_2)]$ in (37) is larger. Furthermore, when the voltage sensitivity of the capacitance is increased, the product C_0R_s also increases. The over-all effect on the product $\bar{\gamma}Q_n$ could be a decrease with increased voltage sensitivity. If $\bar{\gamma}Q_n$ is lower with increased voltage sensitivity, g_T will undoubtedly be lower because the other

[11] J. C. Irvin, "Resistivity of bulk silicon and of diffused layers in silicon," *Bell Sys. Tech. J.*, vol. 41, pp. 387–410; March, 1962.

[12] T. M. Hyltin and K. L. Kotzebue, "A solid-state microwave source from reactance-diode harmonic generators," IRE Trans. on Microwave Theory and Techniques, vol. MTT-9, pp. 73–78; January, 1961.

factor, $(1 - \gamma_{n+1}/\gamma_{n-1})$, in g_T decreases with increased voltage sensitivity. A theoretical comparison has been made between a type B hyperabrupt junction and an abrupt junction both having breakdown voltages of 8 volts and being used to convert 1 kMc power to 2 kMc. The former junction gives $\bar{\gamma}Q_n \simeq 220$ and $g_T \simeq 74$ per cent, and the latter $\bar{\gamma}Q_n \simeq 400$ and $g_T \simeq 83$ per cent.

However, as pointed out by Hyltin and Kotzebue,[12] their formula (35) was apparently in error because g_T does not approach unity as it should when Q_n approaches infinity. They attributed this error to their small signal approximation. Therefore, the above numerical comparison can only be considered as some indication that hyperabrupt junctions may be unfavorable as harmonic generators.

As in the case of low-noise amplification when the resistance of the p-n junction is negligible compared with other resistances such as contact resistances, bulk resistance, and resistances in the external circuits, hyperabrupt junctions may still prove to be better than abrupt junctions. Under certain conditions, Canick and Yuan[13] did obtain better efficiencies from varactors with higher voltage sensitivities.

VI. Varactors with the Pagoda Structure

The pagoda structure is shown in Fig. 6. In this type of varactor, it is desirable to have the lightly doped side of the junction on the top so that the space-charge region expands mostly toward the surface when the junction is biased in the reverse direction. When reverse bias voltage is increased, x_n moves upward. As x_n passes the plane, $x = x_1$, where the cross-sectional area decreases suddenly, the junction capacitance drops sharply. Fig. 7 shows the capacitance-voltage curves for several pagoda structure varactors. However, these capacitance-voltage characteristics were measured at 0.1 Mc. At high frequencies, no such large capacitance variations were observed. This can be explained by a very rough argument like the following: When $x_n < x_1$, in series with the capacitance ΔC contributed by the region $r_0 \leq r \leq r_1$, there is a resistance ΔR of the order of magnitude of $\rho/(x_1 - x_n)$, where ρ is the resistivity in the n region. At high frequencies, $\Delta R \gg 1/\omega\ \Delta C$ and this high resistance ΔR is shunted out by the capacitance C in the region $r \leq r_0$. Hence only this relatively small capacitance C is measurable at high frequencies. Measurements on several units at frequencies between 0.1 Mc and 1 kMc at zero bias showed that the equivalent series resistance was approximately inversely proportional to frequency and the equivalent series capacitance increased with decreasing frequency at a slower rate than the resistance. The high resistance in the thin layer between x_n and x_1 can be improved by evaporating a thin layer of high conductivity material such as gold on the $x = x_1$ plane as

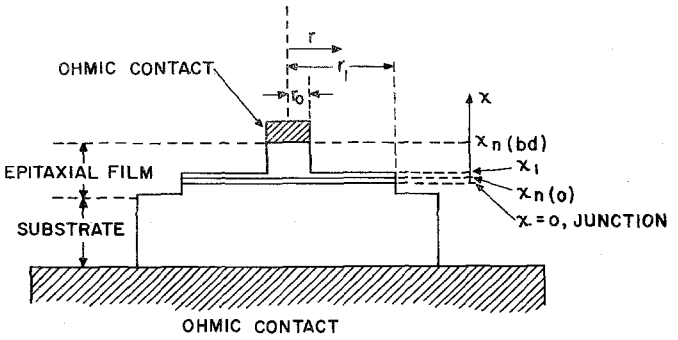

Fig. 6—The cross-sectional view of a pagoda varactor. The dimensions are not shown in proportion.

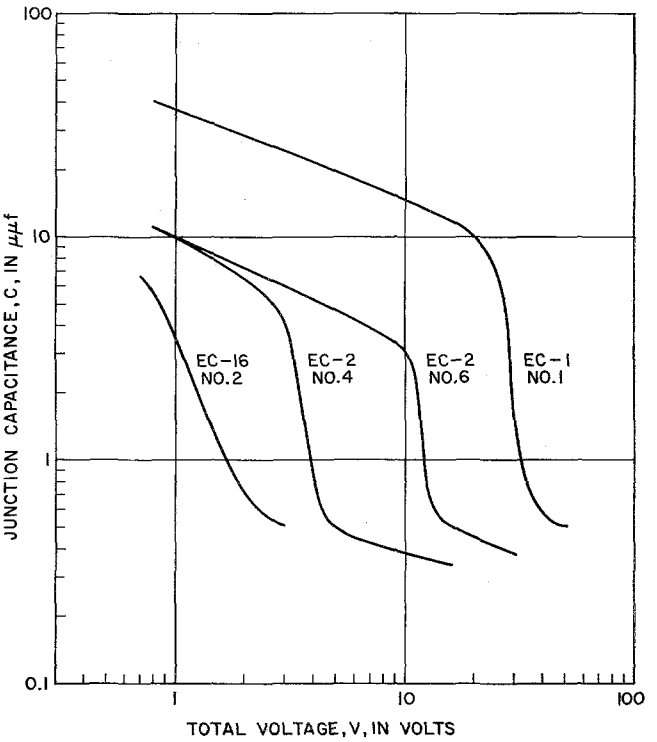

Fig. 7—The capacitance-voltage characteristics of some pagoda varactors measured at 0.1 Mc. The built-in potential is taken to be 0.8 volts.

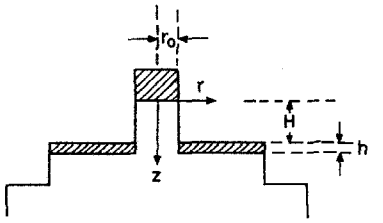

Fig. 8—The pagoda varactor with highly conducting layer evaporated on the $x = x_1$ plane of the varactor shown in Fig. 6.

[13] P. Canick and S. Yuan, "Γ-dependence of varactor frequency doublers," Proc. IRE (*Correspondence*), vol. 50, pp. 1533–1534; June, 1962.

shown in Fig. 8. If this is successfully done, contact can further be made to this evaporated layer to form a type of spacistor. At the present time, we shall consider only the varactor application of this device. Let us assume that the junction capacitance takes only two values and that the device is so driven that

$$\begin{aligned} C &= C_{\max} \qquad (0 \leq \omega_p t \leq p) \\ &\quad C_{\min} \qquad (p \leq \omega_p t \leq \pi). \end{aligned} \tag{38}$$

Then the dynamic quality factor, $\tilde{Q}$, as defined by (12) has a maximum value

$$\tilde{Q}_{\max} = \frac{1}{\omega R_0 C_{\min}\left[1 + \frac{p_Q}{\pi}\left(\frac{C_{\max}}{C_{\min}} - 1\right)\right]\left[\frac{2}{\gamma_Q} - \frac{\gamma_Q}{2}\right]} \tag{39}$$

when p takes a value p_Q given by

$$\tan p_Q(1 + \sin p_Q) - p_Q = \frac{\pi}{\left(\frac{C_{\max}}{C_{\min}} - 1\right)}. \tag{40}$$

The quantity γ_Q in (39) is obtained by substituting p_Q in the expression for $|\gamma_1|$,

$$|\gamma_1| = \frac{2 \sin p}{p + \frac{\pi}{\left(\frac{C_{\max}}{C_{\min}} - 1\right)}}. \tag{41}$$

The resistance between the evaporated layer and the top ohmic contact is found to be

$$R = \rho \frac{H + h}{\pi r_0^2} \cdot \frac{4r_0}{\pi^2 h} \sum_{n=0}^{\infty} \frac{(-1)^n}{(2n + 1)^2} \cos Hy_n \frac{I_0(r_0 y_n)}{I_1(r_0 y_n)} \tag{42}$$

where I_0 and I_1 are the modified Bessel functions of the first kind of order zero and one, respectively, and

$$y_n = \frac{(2n + 1)\pi}{2(H + h)}. \tag{43}$$

The first part on the right-hand side of (43) is the resistance of a corresponding abrupt junction.

To calculate $\tilde{Q}_{\max}$ for the pagoda structure (Fig. 4), the following assumptions are made: 1) $C_{\max}/C_{\min} = 100$; 2) $H + h$ is approximately equal to the space-charge region width at breakdown voltage; 3) h is chosen so that p may satisfy (38) and (40); and 4) $r_0 = \frac{1}{2}$ mil. The calculated $\tilde{Q}_{\max}$ is plotted in Fig. 4 against the breakdown voltage. This curve shows that in high-voltage units, the dynamic quality factor $\tilde{Q}$ in a pagoda structure can be higher than that in a conventional abrupt junction. (This is because in high-voltage units the resistance in the mesa is so high that it dominates the spreading resistance near the evaporated layer.) However, this small improvement in $\tilde{Q}$ has to be paid for with a much more complicated design and fabrication process.

VII. Conclusions

The hyperabrupt junction (Fig. 1) and the pagoda structure (Fig. 6) can both be thought of as ways to increase the relative capacity variation of a varactor, the first by complicating the impurity profile, the second by varying the geometry from more usual diodes. Both these schemes do indeed succeed in improving the nonlinearity coefficients γ_n, defined by $C(t) = C_0[1 + \gamma_1 \cos \omega t + \gamma_2 \cos 2\omega t + \cdots]$. As against a theoretical maximum $|\gamma_1| = 2$, a practical pagoda diode can achieve $|\gamma_1|$ of about 1.8 while a hyperabrupt varactor with a breakdown voltage of 8 volts can boast a ratio as high as 1.02. Abrupt junctions with the same breakdown voltage, for comparison, run considerably lower at about $|\gamma_1| = 0.5$, while graded junctions may be no more than about 0.3.

In spite of the improvement in nonlinearity, the over-all performance may or may not be improved, because of the concomitant reduction in other performance measures, especially the quality factor $Q = 1/\omega R_s C_0$. For instance, in the particular application to low-noise amplification, according to Kurokawa and Uenohara, the figure of merit is taken to be the dynamic quality factor

$$\tilde{Q} = 1/\omega R_s C_0(2/|\gamma_1| - |\gamma_1|/2).$$

When the negative-gradient region of the hyperabrupt junction is made very narrow, the characteristics approach those of a mathematical model we call the "Type A" hyperabrupt junction [Fig. 2(a)] and $\tilde{Q}$ is about the same as that of an abrupt junction (Fig. 4). In other words, the improvement in nonlinearity just about balances off the increased resistance. On the other hand, for a different proportioning of the hyperabrupt grading such that the junction capacitance is inversely proportional to the total voltage across the junction, the dynamic quality factor turns out to be much lower than that of the abrupt junction. The pagoda structure also is lower in $\tilde{Q}$ than the abrupt junction except in very high-voltage units (Fig. 4). A similar result seems to apply to applications as harmonic generators.

Hence, for applications where the dynamic quality factor $\tilde{Q}$ defined by Kurokawa and Uenohara or the transducer gain g_T derived by Hyltin and Kotzebue is the only important factor neither the hyperabrupt nor the pagoda structure is strongly competitive with the abrupt junction. For certain other applications, where the loss in the p-n junction is dominated by the loss in the ohmic contacts, the semiconductor bulk, or the external circuits, the improvement in γ_n might make hyperabrupt or pagoda structures preferable. For instance, in low-frequency diode harmonic generators, the diode loss is normally negligible and the improvement in γ_n can be advantageous.[13]

Acknowledgment

Acknowledgments are due to D. E. Iglesias for his capable assistance in fabricating and measuring these devices, and S. K. Tung for supplying some of the epitaxial films used for pagoda varactors. The authors would also like to thank those colleagues who helped in the various stages of the fabrication of these devices and those who helped prepare this manuscript.